Received: 21 November 2021 | Revised: 7 June 2022 | Accepted: 8 June 2022

DOI: 10.1002/nbm.4787

RESEARCH ARTICLE

NMR IN BIOMEDICINE WILEY

Signal enhancement of hyperpolarized ^{15}N sites in solution—increase in solid-state polarization at 3.35 T and prolongation of relaxation in deuterated water mixtures

Ayelet Gamliel[1,2] | David Shaul[1,2] | J. Moshe Gomori[1] | Rachel Katz-Brull[1,2]

[1]Department of Radiology, Hadassah Medical Organization and Faculty of Medicine, Hebrew University of Jerusalem, Jerusalem, Israel

[2]The Wohl Institute for Translational Medicine, Hadassah Medical Organization, Jerusalem, Israel

Correspondence
Rachel Katz-Brull, Department of Radiology, Hadassah Medical Organization and Faculty of Medicine, Hebrew University of Jerusalem, Jerusalem 9112001, Israel.
Email: rkb@hadassah.org.il

Funding information
European Commission, Grant/Award Number: 858149—AlternativesToGd; Israel Science Foundation, Grant/Award Number: 1379/18

Hyperpolarized ^{15}N sites have been found to be promising for generating long-lived hyperpolarized states in solution, and present a promising approach for utilizing dissolution-dynamic nuclear polarization (dDNP)-driven hyperpolarized MRI for imaging in biology and medicine. Specifically, ^{15}N sites with directly bound protons were shown to be useful when dissolved in D_2O. The purpose of the current study was to further characterize and increase the visibility of such ^{15}N sites in solutions that mimic an intravenous injection during the first cardiac pass in terms of their H_2O:D_2O composition. The T_1 values of hyperpolarized ^{15}N in [$^{15}N_2$]urea and [^{15}N]NH_4Cl demonstrated similar dependences on the H_2O:D_2O composition of the solution, with a T_1 of about 140 s in 100% D_2O, about twofold shortening in 90% and 80% D_2O, and about threefold shortening in 50% D_2O. [^{13}C]urea was found to be a useful solid-state ^{13}C marker for qualitative monitoring of the ^{15}N polarization process in a commercial pre-clinical dDNP device. Adding trace amounts of Gd^{3+} to the polarization formulation led to higher solid-state polarization of [^{13}C]urea and to higher polarization levels of [$^{15}N_2$]urea in solution.

KEYWORDS
ammonium, carbon-13, D_2O, dissolution dynamic nuclear polarization, nitrogen-15, urea

1 | INTRODUCTION

Hyperpolarized ^{15}N sites have been found to be promising for generating long-lived hyperpolarized states in solution and present a promising approach for utilizing dissolution-dynamic nuclear polarization (dDNP)-driven hyperpolarized MRI for imaging in biology and medicine.[1–6] The purpose of the current study was to further characterize and increase the visibility of such ^{15}N sites in solution, specifically for those sites with directly bound deuterium atoms.[1] This work has been done as a preparation for translation of these potentially useful agents to intravenously (IV) injected hyperpolarized compounds. We aimed to provide a basis for predicting the effect of the inevitable mixing of the bolus injection of the hyperpolarized medium (which is D_2O based) with the water-based blood, further to the injection. Only the solvent-protonation-related T_1 shortening effect was tested here, as the interaction with whole blood and the inevitable resultant overall T_1 shortening has been previously reported.[1,2] Two separate directions were investigated: (1) the effect of D_2O concentration in the water solution on the hyperpolarized ^{15}N T_1

Abbreviations: CPS1, carbamoyl-phosphate synthetase 1; dDNP, dissolution-dynamic nuclear polarization; IV, intravenous; MW, microwave.

and (2) the effect of adding trace amounts of Gd^{3+} agent to the polarization formulation on the ^{15}N polarization in the solid state and the T_1 in solution.

Hyperpolarized ^{15}N sites that are bound to exchangeable protons have shown prolonged relaxation time when dissolved in D_2O.[1] However, in a potential medical application, these solutions will have to be injected into the bloodstream, where mixing with non-deuterated water-based blood will lead to a shorter relaxation time. However, upon bolus injection, dilution of the bolus by the total body blood content is not immediate, with increasing dilution with each cardiac recirculation. The first (cardiac) pass of the bolus volume may be recorded and utilized as a diagnostic factor. The same strategy has been used with Gd-based contrast agents on MRI[7] and with other exogenous agents and imaging modalities.[8] Such studies suggest that the IV injected bolus has a peak arterial concentration at about 10 s after the injection on passing through the heart for the first time, before cardiac recirculation, in a human-size body, and a second lower peak at about 30 s after the injection[9] due to the second cardiac pass. During the duration of the first pass, we estimate that the hyperpolarized compound may be surrounded by 80–90% of the original bolus composition mixed with 20–10% volume of blood, respectively. To estimate the effect of such mixing on the T_1 of the hyperpolarized agent during the first pass, when injected as a bolus (in D_2O), we studied the T_1 relaxation of hyperpolarized ^{15}N agents bound to exchangeable protons in various D_2O concentrations in water. To this end, we tested two ^{15}N-labeled agents—[$^{15}N_2$]urea, whose potential as a perfusion agent has been suggested multiple times,[1] and [^{15}N]ammonium chloride, which is not intended for in vivo use and is used here only as a model system with the maximal number of exchangeable protons directly bound to the hyperpolarized ^{15}N site.

In order to optimize the ^{15}N polarization in the solid state one must be able to monitor it in that state. Otherwise, multiple polarization and dissolution experiments are required for this, as previously reported.[1,2] Besides being very costly in terms of liquid helium consumption, such studies consist of additional variables (e.g. solution composition, temperature, duration between the end of the solid-state polarization and the measurement in solution), and are therefore prone to further errors. Ideally, one would like to have a solid-state ^{15}N NMR probe within the dDNP device; however, this is not a very common experimental set-up and has been reported in the literature only once.[10] We show here a potential bypass for this problem, originally designed only to show that the sample is in place but which turned out to provide a potential qualitative indication of the solid-state ^{15}N polarization.

2 | MATERIALS AND METHODS

2.1 | Chemicals

The OX063 radical (GE Healthcare, Chalfont Saint Giles, UK) was obtained from Oxford Instruments Molecular Biotools (Oxford, UK). [$^{15}N_2$]urea, [^{13}C]urea, [2-^{13}C]glycerol, [$^{13}C_3$]glycerol, and [$^{13}C_6$]D-glucose were purchased from Sigma-Aldrich (Rehovot, Israel). [$^{13}C_6$]2-deoxy-D-glucose was purchased from Omicron Biochemicals (South Bend, IN, USA). [^{15}N]NH_4Cl was purchased from Cambridge Isotope Laboratories (Andover, MA, USA). Gd^{3+} as gadoteric acid–gadoterate meglumine (Dotarem) was obtained from Guerbet (Villepinte, France).

2.2 | Spin polarization

Spin polarization was performed in a dDNP spin polarizer (HyperSense, Oxford Instruments Molecular Biotools) operating at 3.35 T. For [$^{15}N_2$]urea and [^{13}C]urea, the polarization was achieved by irradiating the sample at a microwave (MW) frequency of range of 94.104–94.150 GHz. For [^{15}N]NH_4Cl, the polarization was achieved by irradiating the sample at an MW frequency of 94.116 GHz ($n = 2$) or 94.136 GHz ($n = 21$). Both polarization protocols were carried out with a power of 100 mW for the MW irradiation, at 1.5 K, for about 2 h. The MW source of the spin polarizer was replaced towards the end of the study (prior to acquiring the data shown in Figure 6 later). To eliminate possible differences in MW source frequency calibrations, the [^{13}C]urea irradiation frequencies were referenced to that of [1-^{13}C]pyruvic acid P^+ (the first maximum in the DNP MW intensity profile), as shown in Figure 3 later.

2.3 | NMR spectroscopy

^{15}N NMR spectroscopy was performed using a 5.8 T high resolution NMR spectrometer (RS2D, Mundolsheim, France), equipped with a 10 mm broad-band NMR probe. Hyperpolarized ^{15}N spectra were acquired using a hard pulse with a flip angle of 10°, a repetition time of 5 s, and 16 384 points.

2.4 | Calculation of hyperpolarized [$^{15}N_2$]urea and [^{15}N]NH_4Cl T_1

The T_1 was determined from the decay curve of the hyperpolarized ^{15}N signal at 35–44 °C. Curve fitting was performed using MATLAB (MathWorks, Natick, MA, USA), taking into account the decay of the signal due to the time from the first spectrum and the cumulative effect of the RF pulses, according to

$$A_t = A_0\, e^{-\frac{t}{T_1}}(\cos\theta)^{t/T_R} \quad (1)$$

where A_t is the intensity of the signal at time t, A_0 is the intensity of signal on the first spectrum, t is the time from the first spectrum, T_R is the repetition time (5 s), T_1 is the spin–lattice relaxation time, and θ is the flip angle of the RF pulse excitation (10°).

2.5 | A ^{13}C solid-state tracer

To systematically characterize the polarization of ^{15}N, in the absence of a solid-state probe for ^{15}N in the polarizer, multiple ^{15}N polarizations and dissolutions would have to be performed with a high solid-state polarization, as previously described.[1,2] Unfortunately, the commercial dDNP device used here, which is common in non-clinical dDNP laboratories, can only detect ^{13}C polarization in the solid state. This prohibits monitoring the solid-state polarization build-up of other nuclei and also puts the procedure and the instrument at risk, as one cannot monitor the MW irradiation process or the presence of the polarization cup within the polarization chamber. The latter could lead to spraying water in the polarization chamber, which will be immediately frozen (at 4 K) and prevent the instrument's operation.

To resolve the above problems, we looked for a ^{13}C-labeled agent that could be added to the ^{15}N agent's polarization formulation, and mark the progress of MW irradiation and the presence of the polarization cup in the polarization chamber.

Several attempts to use pH neutral compounds such as [2-^{13}C]glycerol, [$^{13}C_3$]glycerol, [$^{13}C_6$]D-glucose, and [$^{13}C_6$]2-deoxy-D-glucose for this purpose did not yield detectable ^{13}C polarization in the solid state at sufficiently short time (about 15 min) and low quantity (<20 mg formulation). As the main agent we wished to investigate was [$^{15}N_2$]urea, we also investigated the use of [^{13}C]urea for this purpose.

2.6 | Composition of polarization formulations

2.6.1 | Formulation 1—[$^{15}N_2$]urea without Gd^{3+}

A typical formulation for [$^{15}N_2$]urea polarization consisted of OX063, 3.88 mg (15.0 mM); [$^{15}N_2$]urea, 79.4 mg; and 181.0 μL of a D_2O:glycerol mixture at a respective ratio of 0.6:0.4. The concentration of urea in this formulation was 4.42 μmol/mg formulation.

2.6.2 | Formulation 2—[^{13}C]urea without Gd^{3+}

A typical formulation for [^{13}C]urea polarization consisted of OX063, 3.48 mg (15.1 mM); [^{13}C]urea, 70.4 mg; and 161.9 μL of a D_2O:glycerol mixture at a respective ratio of 0.6:0.4. The concentration of urea in this formulation was 4.40 μmol/mg formulation.

2.6.3 | Formulation 3—[$^{15}N_2$]urea with Gd^{3+}

A typical formulation for [$^{15}N_2$]urea polarization in the presence of Gd^{3+} consisted of OX063, 3.46 mg (15.0 mM); [$^{15}N_2$]urea, 70.86 mg; and 186.58 mg of a mixture of 1.3 mM Gd^{3+} in D_2O:glycerol at a respective ratio of 0.6:0.4. The total concentration of urea in this formulation was 3.8 μmol/mg formulation.

2.6.4 | Formulation 4—[^{13}C]urea with Gd^{3+}

A typical formulation for [^{13}C]urea polarization in the presence of Gd^{3+} consisted of OX063, 2.64 mg (14.9 mM); [^{13}C]urea, 53.69 mg; and 141.28 mg of a mixture of 1.3 mM Gd^{+3} in D_2O:glycerol at a respective ratio of 0.6:0.4. The concentration of urea in this formulation was 4.5 μmol/mg formulation.

2.6.5 | Combinations of Formulations 1–4 for studies of [$^{15}N_2$]urea

A typical formulation loaded into the dDNP cup for studies without Gd^{3+} consisted of 20.25 mg of Formulation 1 combined with 19.93 mg of Formulation 2. A typical formulation loaded into the dDNP cup for studies in the presence of Gd^{3+} consisted of 19.85 mg of Formulation 3 combined with 12.25 mg of Formulation 4. The [^{13}C]urea formulations were added to confirm that the cup is in the correct position in the polarization device and that the MW source is working, by monitoring the ^{13}C build-up in the solid state (i.e., as a ^{13}C solid-state tracer).

2.6.6 | Formulation 5—combined formulation of [^{13}C]urea and [$^{15}N_2$]urea without Gd^{3+}

This formulation consisted of 96.90 mg of Formulation 1 combined with 96.45 mg of Formulation 2.

2.6.7 | Formulation 6—combined formulation of [^{13}C]urea and [$^{15}N_2$]urea with Gd^{3+}

This formulation consisted of 72.35 mg of Formulation 3 combined with 71.68 mg of Formulation 4.

2.6.8 | Formulation 7

A typical formulation for [^{15}N]NH_4Cl polarization consisted of OX063, 2.67 mg (14 mM); [^{15}N]NH_4Cl, 26.16 mg; 74.2 μL D_2O; and 40.19 mg glycerol. The total concentration of NH_4Cl in this formulation was 3.18 μmol/mg formulation.

2.6.9 | Addition of a ^{13}C tracer to Formulation 7

In some of the experiments, [$^{13}C_6$,D_7]D-glucose (15–18 mg) was added as ^{13}C solid-state marker to the [^{15}N]NH_4Cl formulation. In other experiments the [^{15}N]NH_4Cl formulation was added to a cup that had a plastic-wrapped droplet of [1-^{13}C]pyruvic acid formulation attached to the bottom (not mixed with the [^{15}N]NH_4Cl formulation), for the same purpose. These experiments were carried out before establishing [^{13}C]urea as a useful ^{13}C solid-state tracer.

2.7 | Fast dissolution

For studies in solution, following polarization, the formulation was dissolved in 4 mL of D_2O:H_2O mixtures and directly injected into a 10 mm NMR tube located inside the NMR spectrometer. A heating tape was wrapped around the dissolution discharge line and set to 40 °C. The concentration ranges of urea and NH_4Cl in the dissolution media were 21–48 mM and 16–20 mM, respectively.

2.8 | Temperature monitoring during ^{15}N hyperpolarization decay in the NMR spectrometer

An NMR compatible temperature sensor was fixed inside the NMR tube, at a position corresponding to the middle of the NMR detection probe, to monitor the temperature throughout the experiment (OSENSA, Burnaby, British Columbia, Canada).

2.9 | Statistical analysis

Statistical analysis was calculated with Excel (Microsoft, Ra'anana, Israel). Significance for all comparisons was tested using a one-tailed, non-paired Student *t*-test.

3 | RESULTS

3.1 | The effect of D_2O concentration and the presence of Gd^{3+} on [$^{15}N_2$]urea T_1 at body temperature

Figure 1 and Table S1 show that, as regards the effect of D_2O percent in the water solution on the T_1 of [$^{15}N_2$]urea, reducing the concentration of D_2O from 100% to 90% and 80% led to a T_1 shortening of about twofold (from 144 ± 57 s ($n = 4$) to 75 ± 12 s ($n = 3$) and 86 ± 20 s ($n = 3$),

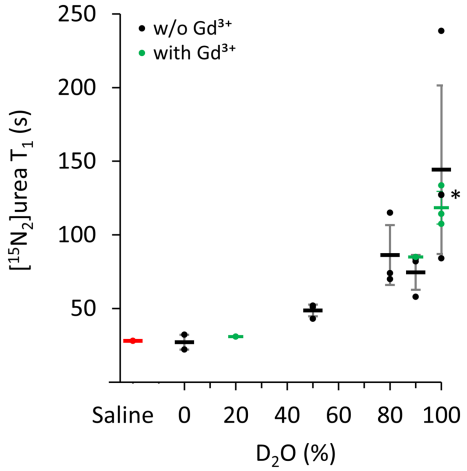

FIGURE 1 The T_1 of ^{15}N in [$^{15}N_2$]urea in D_2O:H_2O mixtures with and without Gd^{3+}. Each point represents an individual T_1 measurement of hyperpolarized [$^{15}N_2$]urea in saline (H_2O based, red), or in various concentrations of D_2O in H_2O, with Gd^{3+} or without. The red, green, and black bars are the respective means. The standard deviations are shown in grey. Further information on the individual experiments is provided in Table S1. *In this condition (100% D_2O without Gd^{3+}) there were two measurements with the same T_1 value (127 s), $n = 4$ altogether.

TABLE 1 Polarization parameters, T_1 in solution, and enhancement factor of hyperpolarized stable-isotope-labeled urea

Gd^{3+} concentration in the formulation (mM)	Sample number in Figures 4 & 5	MW irradiation frequency (GHz)	Concentration of [$^{15}N_2$]urea in the solution (mM)	^{15}N enhancement factor in solution
1.3	1	94.130	18.9	22 456
	2	94.140	18.7	18 441
	3	94.150	18.5	14 505
	Average ± standard deviation			18 467 ± 3246*
0	4	94.140	24.2	10 749
	5	94.140	22.4	11 025
	6	94.140	22.4	9 761
	Average ± standard deviation			10 512 ± 543

[a]a.u., arbitrary units. The polarization levels of [^{13}C]urea in a.u. were normalized to the mass in the cup. The levels of the normalized polarizations are reported at 75 min of polarization due to malfunction of the MW irradiation source after that time on one of the time courses; see also Figure 4.
*$p = 0.013$.
**$p = 0.012$.
***$p = 0.034$. All comparisons made with a one-tailed, non-paired Student t-test.

TABLE 1 (Continued)

Gd^{3+} concentration in the formulation (mM)	^{15}N polarization in solution (%)	[$^{15}N_2$]urea T_1 in solution (s)	Polarization level of [^{13}C]urea after 75 min of polarization (a.u.)[a]
1.3	7	114	818
	5.8	134	696
	4.6	107	335
	5.8 ± 1.0**	118 ± 11	616 ± 205***
0	3.4	127	259
	3.5	127	255
	3.1	84	258
	3.3 ± 0.2	113 ± 20	257 ± 2

[a]a.u., arbitrary units. The polarization levels of [^{13}C]urea in a.u. were normalized to the mass in the cup. The levels of the normalized polarizations are reported at 75 min of polarization due to malfunction of the MW irradiation source after that time on one of the time courses; see also Figure 4.
*$p = 0.013$.
**$p = 0.012$.
***$p = 0.034$. All comparisons made with a one-tailed, non-paired Student t-test.

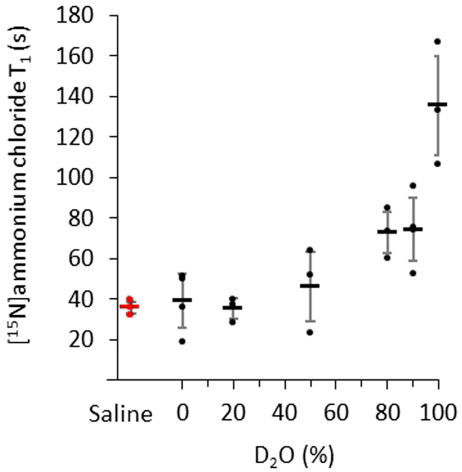

FIGURE 2 The T_1 of ^{15}N in [^{15}N]NH_4Cl in D_2O:H_2O mixtures. Each point represents an individual T_1 measurement of [^{15}N]NH_4Cl in saline (red) or in different concentrations of D_2O in H_2O (black). The bars represent the means (red and black respectively). The standard deviations are shown in grey. Further information on the individual experiments is provided in Table S2.

respectively). A reduction to 50% D_2O led to a T_1 shortening of about threefold (from 144 ± 57 s ($n = 4$) to 49 ± 4 s ($n = 3$)). Figure 1, Table 1, and Table S1 show that the addition of Gd^{3+} to the formulation for polarization did not change the T_1 relaxation time in solution, as determined in 100% D_2O to avoid solvent proton relaxation effects, (144 ± 57 s ($n = 4$) without Gd^{3+} and 118 ± 11 s ($n = 3$) with Gd^{3+}).

3.2 | The effect of D_2O concentration on [^{15}N]NH_4Cl T_1 at body temperature

Figure 2 and Table S2 show that, as regards the effect of D_2O percent in the water solution on the T_1 of [^{15}N]NH_4Cl, reducing the concentration of D_2O from 100% to 90% and 80% D_2O led to a T_1 shortening of about 1.8-fold (from 136 ± 26 s ($n = 3$) to 75 ± 15 s ($n = 3$) and 73 ± 10 s ($n = 3$), respectively). A reduction to 50% D_2O led to a T_1 shortening of about 2.9-fold (from 136 ± 26 s ($n = 3$) to 46 ± 17 s ($n = 3$)).

3.3 | A ^{13}C solid-state tracer for ^{15}N polarization on a dDNP device with a ^{13}C only spectrometer

Studies with multiple ^{13}C-labeled traces (Section 2) did not yield ^{13}C solid-state SNR at sufficiently short time (~15 min) and sufficiently low quantity (<20 mg formulation). However, studies with [^{13}C]urea showed promising results. To optimize the performance of [^{13}C]urea as a solid-state tracer we first characterized its MW irradiation profile. Such studies were done on large samples (typically 180 mg to 260 mg formulations) using irradiation intervals of 4 min for every frequency point. Figure 3 shows the MW irradiation profile of a [^{13}C]urea formulation that did not contain Gd^{3+} ions and of formulations that contained 0.7 mM, 1.3 mM, and 2.3 mM Gd^{3+} ions (as gadoterate meglumine). It can be seen that the addition of Gd^{3+} shifts the center of the first lobe of this profile and narrows it. The range of Gd^{3+} concentrations that was tested here resulted in similar MW irradiation profiles. The formulation with 1.3 mM Gd^{3+} (a Gd^{3+} concentration previously found favorable for [$^{13}C_6$,D_7]D-glucose polarization as well[11]) was tested three times to ensure reproducibility of the profile.

In order to choose the best formulation for the solid-state [^{13}C]urea tracer, we recorded the solid-state build-up of these formulations. The formulations that contained Gd^{3+} at concentrations of 0.7 mM and 1.3 mM showed a 2–2.5 times higher polarization level and an apparent shorter build-up time constant (Table 2: 76 and 73 min for 0.7 and 1.3 mM Gd^{3+}, respectively, versus 108 min without Gd^{3+}). However, while the build-up time is about the same in both formulations that contained Gd^{3+}, the maximal polarization level was higher for the formulation that consisted of 1.3 mM Gd^{3+}. The formulation that contained 2.3 mM Gd^{3+} showed a lower maximal polarization level on the MW intensity profile. Although this profile is shown in Figure 3, this lower intensity is not apparent due to the normalization of the data. For this reason, its use was discontinued and the formulation with 1.3 mM $Gd^{3+}$was selected for further studies.

Figure 4 shows the solid-state ^{13}C polarization build-up characteristics of [^{13}C]urea when polarized together with formulations of [$^{15}N_2$]urea, without or with Gd^{3+} (a combination of Formulations 1 and 2 or Formulations 3 and 4, respectively, see Section 2). Each combined formulation was polarized for the duration shown in Figure 4 and then rapidly dissolved and transferred to the NMR tube, which was situated inside the spectrometer, to record the hyperpolarized ^{15}N signal of [$^{15}N_2$]urea in solution. The enhancement factor of these samples in solution is provided in Figure 5 and Table 1. On one of the polarizations with Gd^{3+} (no 1 in Figure 4), the MW source stopped irradiating after 75 min due to malfunction

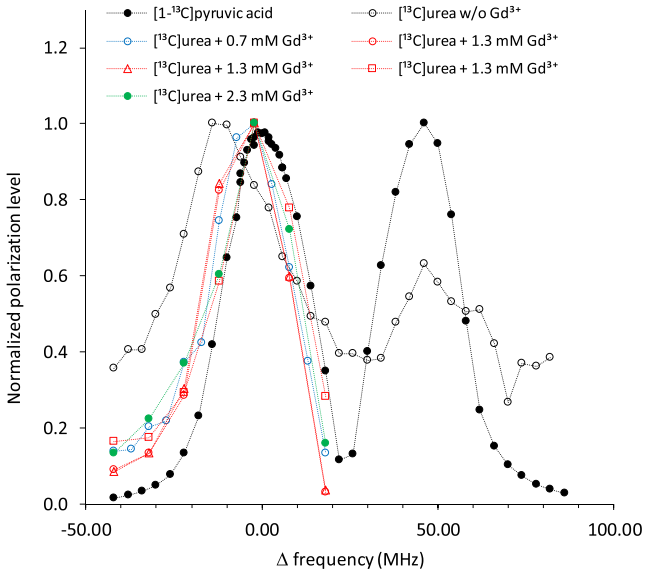

FIGURE 3 MW irradiation profiles of [^{13}C]urea formulations, with and without Gd^{3+}. Values are processed as magnitude and are therefore all positive. Each profile was normalized to its highest point. Further information on the individual experiments is provided in Tables S3 and S4. w/o, without. The MW irradiation profile of [1-^{13}C]pyruvic acid was added to the plot as a reference for irradiation frequency. The P^+ of [1-^{13}C] pyruvic acid was assigned to 0 GHz (the actual frequency was 94.132 GHz). This was done to (1) emphasize the difference in irradiation frequencies between the profiles, (2) accommodate a change in MW source towards the end of the study and eliminate possible changes in MW source frequency calibrations (Figure 6), and (3) allow other centers to follow up the same protocol if the MW source frequency calibrations are not aligned.

TABLE 2 The effect of Gd^{3+} in the polarization formulation on the solid-state polarization build-up time constants and on the maximal polarization level of [^{13}C]urea

Gd^{3+} concentration in the formulation (mM)	[^{13}C]urea build-up time constant (min)	[^{13}C]urea maximal polarization level (a.u.)[a]	Number of samples tested
1.3	73 ± 4[b]	4895 ± 164[c]	3[d]
0.7	76 ± 16	4115 ± 411[e]	3[d]
w/o	108 ± 3	1946 ± 604	2[d,f]

Further information on the individual experiments is provided in Table S3.
w/o, without.
[a]The polarization level was normalized to the mass of formulation in the cup.
[b]$p = 0.002$, comparing the results w/o Gd^{3+} to 1.3mM Gd^{3+}.
[c]$p = 0.004$, comparing the results w/o Gd^{3+} to 1.3 mM Gd^{3+}. All comparisons made with a one-tailed, non-paired Student *t*-test.
[d]The build-up was recorded using MW irradiation at 94.136 GHz.
[e]$p = 0.017$ comparing the results w/o Gd^{3+} to 0.7 mM Gd^{3+}.
[f]The build-up was recorded using MW irradiation at 94.120 GHz.

that was later confirmed. This malfunction likely led to the decrease in ^{13}C solid-state polarization level that was observed in the later time points of this time course.

The experiments marked 1–3 in Figure 4 (which were performed with formulations that contained 1.3 mM Gd^{3+}) were performed with various MW irradiation frequencies in an attempt to optimize the hyperpolarized ^{15}N signal in solution (the enhancement factor reported in Table 1). The variability in ^{15}N enhancement factor (Table 1) and solid-state ^{13}C polarization (Figure 4) of these samples is likely attributable to this variation in irradiation frequency.

The increase in solid-state build-up level and shorter build-up times shown in Figure 4 and Table 2 for the formulations that contained Gd^{3+} was favorable for tracing the process of MW irradiation and for making sure the cup with the polarization formulation was in the polarization chamber. As shown in Figure 1 and Table 1, the minute concentration of 6–7 μM Gd^{3+} dissolved in the hyperpolarized medium (1.3 mM × ~20 μL/4 mL) did not shorten the T_1 of the hyperpolarized ^{15}N site. We then examined the polarization level of [$^{15}N_2$]urea in these studies (Table 1). To our surprise, it appeared that the conditions that benefitted [^{13}C]urea polarization in the solid state also benefitted the

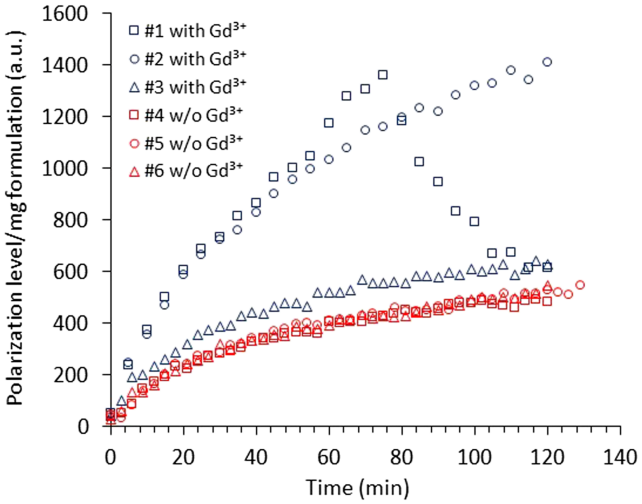

FIGURE 4 Solid-state polarization build-up time courses of [^{13}C]urea when polarized together with formulations of [$^{15}N_2$]urea, without or with Gd^{3+} (1.3 mM). Each time course is marked with a different marker; formulations that contained Gd^{3+} are colored dark blue and formulations without Gd^{3+} are colored red. The time course number corresponds to the experimental description given in Table 1. Note that Samples 1–3 were irradiated at different MW frequencies (Table 1). Further information on the individual experiments is provided in Table S3. w/o, without.

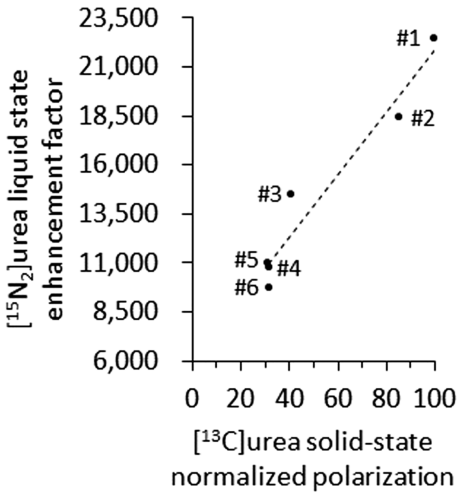

FIGURE 5 Correlation between the solid-state polarization level of [^{13}C]urea and the polarization of [$^{15}N_2$]urea in solution. Each point represents the solid-state ^{13}C polarization level of [^{13}C]urea and the enhancement factor of [$^{15}N_2$]urea in solution (of the same formulation). For convenience, the ^{13}C polarization level was normalized here to the highest a.u. value. A linear fit was achieved with $a = 159$ and $b = 6016$ ($R^2 = 0.94$).

polarization level of ^{15}N in solution (Figure 5 and Table 1). When examining the [^{13}C]urea solid-state polarizations at 75 min (Figure 4, before the MW source malfunction on polarization build-up 1) in comparison with the polarization of [$^{15}N_2$]urea in solution derived from the same samples and polarization processes, it can be seen that these polarization levels correlate (Figure 5). The irradiation at various MW frequencies was serendipitous in revealing this correlation.

To make sure that, when irradiating at the same MW frequency, the variability is lower among build-up time courses for formulations that consist of both [^{13}C]urea and [$^{15}N_2$]urea, we performed another set of experiments. This time we recorded build-up time courses from the same sample, which was situated at exactly the same place in the polarizer. In this set of experiments only two (large) samples were used (Formulations 5 and 6). Three build-up time courses were recorded from each sample. The polarization was given a day to relax in between recordings, while the sample remained inside the polarizer. Figure 6 and Table 3 show that in this set of recordings the variability in build-up time constant and maximal polarization is lower. Of note, this set of experiments was carried out with a different MW source from the rest of the experiments reported here.

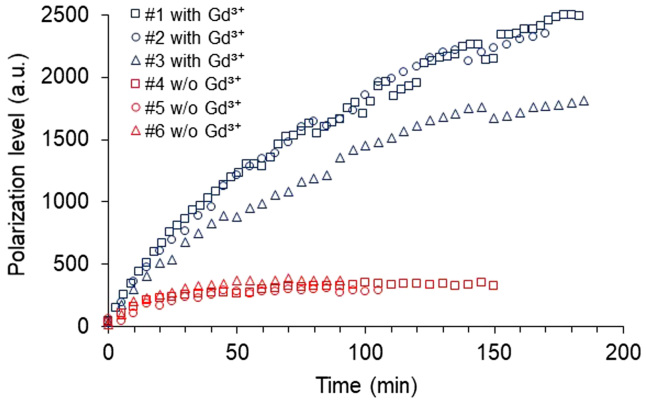

FIGURE 6 Polarization build-up time course for formulations that contain both [^{13}C]urea and [$^{15}N_2$]urea, with or without Gd^{3+}. Each set of time courses (with or without Gd^{3+}) was recorded from a single sample, which remained in the polarizer in between recordings. Irradiation was performed with the same MW frequency for all time courses (94.104 GHz) with a power of 10 mW. w/o, without.

TABLE 3 The effect of Gd^{3+} in the polarization formulation on the solid-state polarization build-up time constants and on the maximal polarization level of [^{13}C]urea in formulations that contain both [^{13}C]urea and [$^{15}N_2$]urea

Gd^{3+} concentration in the formulation (mM)	[^{13}C]urea build-up time constant (min)[a]	[^{13}C]urea maximal polarization level (a.u.)[a,b]	Number of samples tested
1.3	89 ± 4[c]	2555 ± 355[d]	3
w/o	19 ± 2	333 ± 31	3

[a]The build-up time courses were recorded using MW irradiation at 94.104 GHz with a power of 10 mW.
[b]The polarization level was normalized to the mass of formulation in the cup.
w/o, without. Comparing the results w/o Gd^{3+} with 1.3 mM Gd^{3+}: [c] $p = 5.6 \times 10^{-4}$; [d] $p = 1.0 \times 10^{-5}$. Both comparisons made with a one-tailed, non-paired Student *t*-test.

The MW frequency was adjusted with respect to the P^+ of [1-^{13}C]pyruvic acid (based on the data shown in Figure 3). In this set of experiments, to save on liquid helium, the irradiation was performed with a power of 10 mW. This is in contrast to the all other measurements reported here, which were carried out with a power of 100 mW. In our experience, this reduction in irradiation power does not change the polarization of [1-^{13}C]pyruvic acid. To the best of our knowledge, the effect of this change is as yet unknown for other compounds.

As opposed to the studies using 100 mW irradiation power that were done on formulations that contained only [^{13}C]urea and not [$^{15}N_2$]urea, Table 3 shows that the build-up time constant was shorter for the sample that did not contain Gd^{3+}. The maximal polarization was still higher for the samples that contained Gd^{3+}, with a larger increase upon 1.3 mM Gd^{3+} doping (7.7-fold in Table 3 versus 2.5-fold in Table 2).

4 | DISCUSSION

To the best of our knowledge, this is the first study reporting the use of Gd^{3+} doping of the polarization formulation for enhancing ^{15}N polarization. We note that in the solid state the concentration of Gd^{3+} is high and therefore affects polarization build-up, most likely through modulation of polarization transfer mechanisms already described before.[12–14] However, in the resulting hyperpolarized solution, the concentration of Gd^{3+} is much lower (6–7 μM) than in the formulation for polarization. The concentration of Gd^{3+} in the solutions studied here is also much lower than the concentration used in MRI studies to relax blood/body water protons (about 2 mM, considering a dose of 20 mL (0.5 M) and a blood volume of 5 L). This likely explains the finding that the T_1 values of hyperpolarized [$^{15}N_2$]urea in solution were similar with or without Gd^{3+} in the polarization formulation. Specifically for [$^{15}N_2$]urea, it was found that the addition of minute amounts of Gd^{3+} to the formulation led to an almost two-fold increase in the enhancement factor of [$^{15}N_2$]urea in solution (Table 1) without deleterious effects on the T_1 in solution (Table 1).

We note that a range of MW frequencies was used for studying the ^{13}C polarization in the solid state (94.104–94.150 GHz) and the ^{15}N T_1 and enhancement factor in solution (94.116–94.150 GHz), as shown in Tables S1, S2, and S3. Clearly, the MW irradiation frequency could affect the polarization level of the hyperpolarized site. However, it is unrelated to determinations of T_1 in solution. We have further shown that, upon irradiation at a single MW frequency, the variation in solid-state polarization characteristics is small (Figure 6 and Table 3).

As regards the study of T_1 of ^{15}N sites in H_2O:D_2O mixtures, it can be seen that decreasing the concentration of D_2O (and in parallel increasing the concentration of H_2O) leads to shorter T_1 for both [$^{15}N_2$]urea and [^{15}N]NH_4Cl, in a similar manner. This finding is in agreement with our previous report on ^{15}N sites that are bound to exchangeable protons in solutions of pure D_2O and H_2O.[1] However, with 90% or 80% D_2O, the T_1 values of both compounds were still long (>70 s). As hyperpolarized injections are done as a bolus, and assuming an injection of the hyperpolarized ^{15}N-labeled compound in 100% D_2O, it is likely that during the first pass the concentrations of D_2O in the hyperpolarized bolus will be in this range (80–90%) and therefore the visibility time of hyperpolarized [$^{15}N_2$]urea and [^{15}N]NH_4Cl in blood will likely benefit from the bound deuterons. In this respect, it is worth noting that the T_1 in whole blood will be further impacted by blood-borne agents such as divalent ions and oxygen. The T_1 of [$^{15}N_2$]urea in whole blood was previously determined to be about 10 s.[1] As a reference, we note that the T_1 of [^{15}N]nitrate, which has no bound protons, in whole blood, was previously reported to be about 30 s.[2] For preclinical imaging in small animals with heart rates of 300–400 beats per minute, the first pass would be much faster than in human subjects and therefore the imaging should be carried out fast as well. This is in agreement with the need to image fast on hyperpolarized MRI.

It is interesting that similar effects (T_1 shortening of about twofold in mixtures of 90% or 80% D_2O and T_1 shortening of about threefold in mixtures of 50% D_2O) have been observed for both compounds: urea and the ammonium ion. This similarity is in contrast to the fact that the former has two exchangeable proton positions and the latter has four. This finding may suggest that the additional interaction with the third and the fourth protons in ammonium chloride adds little to the T_1 relaxation time constant.

Urea is an agent that is safe to use,[15] and stable-isotope-labeled urea analogs have been used in pre-clinical dDNP studies.[16–19] However, [^{15}N]NH_4Cl was studied here mainly as a model system that could validate the results obtained with [$^{15}N_2$]urea, as both consist of exchangeable protons directly bound to ^{15}N and have previously shown prolongation of the ^{15}N T_1 upon dissolution in D_2O.[1] NH_4Cl is not recommended for development as an MRI contrast agent. NH_4Cl is a systemic and urinary acidifying agent that is converted to ammonia and hydrochloric acid through oxidation by the liver. Although IV injection of NH_4Cl is a treatment option for severe cases of metabolic alkalosis,[20] it is generally poorly tolerated due to adverse effects including encephalopathy, metabolic acidosis, and ammonia toxicity.[20–22] The LD_{50} for IV injection of NH_4Cl to rats is 7–10 mmol/kg.[23,24] To the best of our knowledge, further toxicity data and the no-observed-adverse-effect level have not been reported for IV injection of this compound. The physiological concentration of NH_4^+ in the blood is estimated to be between 11 and 50 μM,[25] which is about 1000 times lower than the concentrations used in this study (16–20 mM), further limiting the potential use of this compound as a hyperpolarized MRI agent.

Nevertheless, it is conceivable that hyperpolarized [^{15}N]NH_4Cl could be used in a number of ex vivo studies in the investigation of nitrogen metabolism, such as the following. (1) To observe NH_4^+ and NH_3 metabolism (for example, in the glutamate–glutamine interconversion). (2) To study metabolism relating to the urea cycle. NH_4^+ ions are actively transported by RhBG[26] and are converted to carbamoyl phosphate by carbamoyl-phosphate synthetase (CPS1).[25,27] CPS1 is the rate limiting enzyme in the urea cycle in liver mitochondria[25] and is also useful in diagnosing hepatocellular carcinoma[28] (using the antibody HepPar1[29]). (3) To study transport and viability in the kidney, where NH_4^+ ions enter the collecting duct via NH_4^+/K^+/ATPase.[30] Moreover, the transport of NH_4^+ by various kidney cells[30] and its secretion may be studied using hyperpolarized [^{15}N]NH_4Cl as a marker. The optimization of ^{15}N polarization and the characterization of the T_1 of this agent in various H_2O:D_2O mixtures are likely useful for such potential studies.

As the commercial polarizer available in our laboratory (and in most other hyperpolarized MR laboratories) can only monitor the polarization of ^{13}C in the solid state, we needed a ^{13}C marker within the sample to both (1) mark that the polarization cup has reached the polarization cavity—to confirm that the dissolution stick will lock into the cup during the dissolution process—and (2) verify that the MW source is indeed working throughout the polarization time.

[^{13}C]urea was found to be a useful marker for MW irradiation and the presence of the polarization cup in the polarization chamber. Surprisingly, it was also found that the [^{13}C]urea solid-state polarization was a useful qualitative reporter for [$^{15}N_2$]urea polarization. This may alleviate the need for solid-state ^{15}N polarization monitoring in further studies. However, the one sample in which the MW source stopped irradiating about 1 h prior to dissolution (Sample 1, Figure 4) suggested that the T_1 values of the two nuclei are not the same in the solid state. While the ^{13}C polarization decayed after the end of irradiation, the ^{15}N polarization, as evidenced by the liquid-state polarization (Figure 5), apparently did not decay or did not decay to the same extent. This suggests that the solid-state T_1 of the ^{15}N sites investigated here is longer than the ^{13}C site of [^{13}C]urea (in agreement with the difference between their T_1 values in solution). This observation warrants further investigation and suggests the potential of such compounds to preserve polarization if storage of the polarization is required.[31–33] By fitting the decay of the polarized signal of Sample 1 in Figure 4 and taking into account the effect of 5° excitation pulses, the T_1 of [^{13}C]urea in the solid state was calculated to be about 48 min (Supporting Figure S1). Conceivably, the ^{15}N T_1 of [$^{15}N_2$]urea is longer than this.

Previously, we reported a polarization of 5.1% for [$^{15}N_2$]urea in D_2O.[1] We show here that this polarization can be increased 1.4-fold at 3.35 T by adding Gd^{3+} ions to the polarization formulation (reaching 7% polarization in solution). For [^{15}N]sodium nitrate a lower polarization of 1% was previously reported in solution.[2] It remains to be seen whether the measures investigated here for [$^{15}N_2$]urea and [^{13}C]urea solid-state polarization will be useful also for [^{15}N]sodium nitrate polarization.

In summary, the current studies show promise for an increase in ^{15}N hyperpolarization and suggest prolonged visibility of such hyperpolarized agents in the blood during the first pass following a bolus IV injection (in D_2O).

ACKNOWLEDGEMENT

This study has received funding from the European Commission, Grant/Award 858149—AlternativesToGd, and from the Israel Science Foundation, Grant/Award 1379/18.

DATA AVAILABILITY STATEMENT

The data that support the findings of this study are available from the corresponding author upon reasonable request.

ORCID

Rachel Katz-Brull https://orcid.org/0000-0003-4850-1616

REFERENCES

1. Harris T, Gamliel A, Uppala S, et al. Long-lived ^{15}N hyperpolarization and rapid relaxation as a potential basis for repeated first pass perfusion imaging—marked effects of deuteration and temperature. *ChemPhysChem*. 2018;19(17):2148-2152. doi:10.1002/cphc.201800261
2. Gamliel A, Uppala S, Sapir G, et al. Hyperpolarized [^{15}N]nitrate as a potential long lived hyperpolarized contrast agent for MRI. *J Magn Reson*. 2019;299:188-195. doi:10.1016/j.jmr.2019.01.001
3. Durst M, Chiavazza E, Haase A, Aime S, Schwaiger M, Schulte RF. Alpha-trideuteromethyl ^{15}N glutamine: a long-lived hyperpolarized perfusion marker. *Magn Reson Med*. 2016;76(6):1900-1904. doi:10.1002/mrm.26104
4. Jiang WN, Lumata L, Chen W, et al. Hyperpolarized ^{15}N-pyridine derivatives as pH-sensitive MRI agents. *Sci Rep*. 2015;5:9104. doi:10.1038/srep09104
5. Suh EH, Park JM, Lumata L, Sherry AD, Kovacs Z. Hyperpolarized ^{15}N-labeled, deuterated tris(2-pyridylmethyl)amine as an MRI sensor of freely available Zn^{2+}. *Commun Chem*. 2020;3(1):185. doi:10.1038/s42004-020-00426-6
6. von Morze C, Engelbach JA, Reed GD, et al. ^{15}N-carnitine, a novel endogenous hyperpolarized MRI probe with long signal lifetime. *Magn Reson Med*. 2021;85(4):1814-1820. doi:10.1002/mrm.28578
7. Shiroishi MS, Castellazzi G, Boxerman JL, et al. Principles of T_2^*-weighted dynamic susceptibility contrast MRI technique in brain tumor imaging. *J Magn Reson Imaging*. 2015;41(2):296-313. doi:10.1002/jmri.24648
8. Kucharczyk J, Roberts T, Moseley ME, Watson A. Contrast-enhanced perfusion-sensitive MR imaging in the diagnosis of cerebrovascular disorders. *J Magn Reson Imaging*. 1993;3(1):241-245. doi:10.1002/jmri.1880030136
9. Upton RN. A model of the first pass passage of drugs from iv injection site to the heart—parameter estimates for lignocaine in the sheep. *Br J Anaesth*. 1996;77(6):764-772. doi:10.1093/bja/77.6.764
10. Reynolds S, Patel H. Monitoring the solid-state polarization of ^{13}C, ^{15}N, ^{2}H, ^{29}Si and ^{31}P. *Appl Magn Reson*. 2008;34(3/4):495-508. doi:10.1007/s00723-008-0117-5
11. Harris T, Gamliel A, Nardi-Schreiber A, Sosna J, Gomori JM, Katz-Brull R. The effect of gadolinium doping in [$^{13}C_6$, $^{2}H_7$] glucose formulations on ^{13}C dynamic nuclear polarization at 3.35 T. *ChemPhysChem*. 2020;21(3):251-256. doi:10.1002/cphc.201900946
12. Ardenkjaer-Larsen JH, Macholl S, Johannesson H. Dynamic nuclear polarization with trityls at 1.2 K. *Appl Magn Reson*. 2008;34(3/4):509-522. doi:10.1007/s00723-008-0134-4
13. Banerjee D, Shimon D, Feintuch A, Vega S, Goldfarb D. The interplay between the solid effect and the cross effect mechanisms in solid state ^{13}C DNP at 95 GHz using trityl radicals. *J Magn Reson*. 2013;230:212-219. doi:10.1016/j.jmr.2013.02.010
14. Ravera E, Shimon D, Feintuch A, et al. The effect of Gd on trityl-based dynamic nuclear polarisation in solids. *Phys Chem Chem Phys*. 2015;17(40):26969-26978. doi:10.1039/C5CP04138D
15. Gangolli SD (Ed). *The Dictionary of Substances and Their Effects*. Vol. 7. 2nd ed. Royal Society of Chemistry; 1999:561-562.
16. Qin HC, Zhang V, Bok RA, et al. Simultaneous metabolic and perfusion imaging using hyperpolarized ^{13}C MRI can evaluate early and dose-dependent response to radiation therapy in a prostate cancer mouse model. *Int J Radiat Oncol Biol Phys*. 2020;107(5):887-896. doi:10.1016/j.ijrobp.2020.04.022
17. Farkash G, Markovic S, Novakovic M, Frydman L. Enhanced hyperpolarized chemical shift imaging based on a priori segmented information. *Magn Reson Med*. 2019;81(5):3080-3093. doi:10.1002/mrm.27631
18. Lau AZ, Miller JJ, Robson MD, Tyler DJ. Simultaneous assessment of cardiac metabolism and perfusion using copolarized [1-^{13}C]pyruvate and ^{13}C-urea. *Magn Reson Med*. 2017;77(1):151-158. doi:10.1002/mrm.26106
19. Hansen ESS, Stewart NJ, Wild JM, Stodkilde-Jorgensen H, Laustsen C. Hyperpolarized ^{13}C, $^{15}N_2$-urea MRI for assessment of the urea gradient in the porcine kidney. *Magn Reson Med*. 2016;76(6):1895-1899. doi:10.1002/mrm.26483
20. Palmer BF, Alpern RJ. Disease of the month—metabolic alkalosis. *J Am Soc Nephrol*. 1997;8(9):1462-1469. doi:10.1681/ASN.V891462
21. Lacy CF, Armstrong LL, Goldman MP, Lance LL. *Drug Information Handbook*. 19th ed. Lexi-Comp; 2010.
22. Mathew JT, Bio LL. Injectable ammonium chloride used enterally for the treatment of persistent metabolic alkalosis in three pediatric patients. *J Pediatr Pharmacol Ther*. 2012;17(1):98-103.
23. PubChem compound summary for CID 25517, ammonium chloride. National Center for Biotechnology Information. 2021. Accessed November 13, 2021. https://pubchem.ncbi.nlm.nih.gov/compound/Ammonium-chloride
24. Bohnet M. *Ullmann's Encyclopedia of Industrial Chemistry*. Vol. 3. Wiley-VCH; 2003.
25. Adeva MM, Souto G, Blanco N, Donapetry C. Ammonium metabolism in humans. *Metab Clin Exp*. 2012;61(11):1495-1511. doi:10.1016/j.metabol.2012.07.007
26. Weiner ID, Miller RT, Verlander JW. Localization of the ammonium transporters, RhB glycoprotein and RhC glycoprotein, in the mouse liver. *Gastroenterology*. 2003;124(5):1432-1440. doi:10.1016/S0016-5085(03)00277-4
27. UniProtKB—P31327 (CPSM_HUMAN). UniProt. 2021. Accessed November 15, 2021. https://www.uniprot.org/uniprot/P31327
28. Siddiqui MT, Saboorian MH, Gokaslan ST, Ashfaq R. Diagnostic utility of the HepPar1 antibody to differentiate hepatocellular carcinoma from metastatic carcinoma in fine-needle aspiration samples. *Cancer Cytopathol*. 2002;96(1):49-52. doi:10.1002/cncr.10311

29. Butler SL, Dong H, Cardona D, et al. The antigen for Hep Par 1 antibody is the urea cycle enzyme carbamoyl phosphate synthetase 1. *Lab Invest*. 2008;88(1):78-88. doi:10.1038/labinvest.3700699
30. Weiner ID, Verlander JW. Role of NH_3 and NH_4^+ transporters in renal acid–base transport. *Am J Physiol Renal Physiol*. 2011;300(1):F11-F23. doi:10.1152/ajprenal.00554.2010
31. El Darai T, Cousin SF, Stern Q, et al. Porous functionalized polymers enable generating and transporting hyperpolarized mixtures of metabolites. *Nat Commun*. 2021;12(1):4695. doi:10.1038/s41467-021-24279-2
32. Capozzi A, Cheng T, Boero G, Roussel C, Comment A. Thermal annihilation of photo-induced radicals following dynamic nuclear polarization to produce transportable frozen hyperpolarized ^{13}C-substrates. *Nat Commun*. 2017;8:15757. doi:10.1038/ncomms15757
33. Ji X, Bornet A, Vuichoud B, et al. Transportable hyperpolarized metabolites. *Nat Commun*. 2017;8:13975. doi:10.1038/ncomms13975

SUPPORTING INFORMATION

Additional supporting information can be found online in the Supporting Information section at the end of this article.

How to cite this article: Gamliel A, Shaul D, Gomori JM, Katz-Brull R. Signal enhancement of hyperpolarized ^{15}N sites in solution—increase in solid-state polarization at 3.35 T and prolongation of relaxation in deuterated water mixtures. *NMR in Biomedicine*. 2022;35(11):e4787. doi:10.1002/nbm.4787